Simulations of Galactic Magnetism.

PI: David C. Collins (Florida State University)

1 Objectives and Summary

It has been argued, somewhat facetiously, that there is only one magnetic field line in the universe; ultimately all magnetic environments are connected. Stellar magnetic fields are intimately tied to their local interstellar medium (ISM) by winds and supernovae; the field in the ISM is produced and sustained by the galactic rotation and turbulence; the circumgalactic medium (CGM) provides the boundary conditions for the large scale dynamo, impacting the field in the ISM and delivering magnetic field to the intergalactic medium (IGM). In the proposed work we will use a combination of cosmological and galactic scale simulations to probe the following questions:

1. How and When was the magnetic field of the Galaxy assembled?
2. Where is the field distributed within the galaxy, and how does the assembly, history, and environment affect the distribution and tangling of the magnetic field?
3. What are the observational consequences of this magnetic field distribution?

While these questions pertain to galaxies of all sizes, in this work we will will focus on Milky Way sized (L^*) galaxies and the impact on observable quantities.

We will use two suites of simulations on different time- and size-scales: one *cosmological* spanning 25 Mpc to capture the formation of a Milky Way-sized galaxy cosmological time- and size-scales; and one suite of *isolated galaxy* simulations at 100 kpc that will will simulate the same galaxy with the resolution necessary to capture the turbulence that is crucial for the dynamics of the ISM. The cosmological simulations will be used for the initial and boundary conditions of the isolated galaxy simulations. Simulations will vary the initial mean magnetic field and the amount of field ejected from supernovae.

Simulations will be performed with the open-source code Enzo [12, 22] which has a long history of cosmological and galactic MHD simulations. These simulations will also serve as a development vehicle for Enzo-E, the exascale successor to Enzo [8, 9]. Enzo-E, which is under development and nearly completed, will allow simulations to be performed at a processor count that is not possible for the current Enzo, enabling the dynamic range and resolution necessary to capture the magnetic field evolutions.

We will monitor three quantities in our simulations; the mechanism for field growth, the time scale for growth, and the spatial distribution and correlations of the magnetic field within and around the galaxy.

We will also produce several synthetic observations, most notably synthetic polarized synchrotron and dust emission. The primary areas of study will be the foregrounds for the polarized cosmic microwave background (CMB), and the role of magnetic fields in star forming clouds.

We hypothesize that feedback of magnetic fields from stellar explosions, and subsequent dynamo activity, is responsible for magnetizing the universe. We will address these questions within this framework by:

1. Performing a suite of galaxy formation simulations from cosmological initial conditions, using a set of three subgrid models for magnetic field creation
2. Re-simulate a selection of galaxies at sub-parsec resolution to connect the magnetic fields to the initial and boundary conditions of their birth.
3. Compare synthetic observations of galaxies at each stage to synthetic observations. With these synthetic observations we will address our hypothesis, and provide predictions for future observations.

Observations show that galaxies at $z \simeq 2$ (one-third of the present age of the universe) have magnetic fields that are both organized on large scales and of comparable magnitude to what we see in the Milky

Way today. Organized, dynamically important magnetic fields are also ubiquitous in the interstellar medium of present-day galaxies. The molecular clouds that are the sites of star formation in nearby galaxies form out of this magnetized plasma, and measurements show that these clouds have substantial magnetic fields as well. These magnetic fields are possibly quite important for star formation, which remains one of the most important unsolved problems in astrophysics. While magnetic fields have been observed in all of these astrophysical regimes, and there is a clear sequence of events – galaxies form molecular clouds, which in turn are the sites of star formation – the ways in which magnetic fields tie galaxies to molecular clouds, and thus potentially affect star formation and the initial stellar mass function, are poorly understood theoretically. There is a clear need for a detailed, self-consistent model of cosmological structure formation that can trace the evolution of magnetized gas to the physical scales relevant for star formation.

2 Scientific Motivation

The universe is magnetized on nearly every scale – magnetic fields can be seen in the intergalactic and interstellar medium, in molecular clouds, and in stars. The universe also appears to be magnetized over a wide range of cosmic time, with evidence for magnetic fields observed at high redshift as well as in the local universe. Magnetic fields are dynamically important in many of the observed astrophysical environments, having energy densities that are comparable to (or in equipartition with) other available energy sources, including heat, turbulence, cosmic rays, and radiation. Furthermore, even in situations where magnetic fields are dynamically irrelevant (such as the intergalactic plasma in clusters of galaxies), they are critical for processes such as thermal conduction and particle acceleration. Magnetic fields (and dust pinned to them) also give rise to the majority of the polarized microwave sky, which is an important contaminant for studies of the cosmic microwave background.

2.1 The high-redshift universe

There is evidence that magnetic fields have existed over much of the age of the universe. Observations of high-redshift quasar absorption line spectra show that MgII absorption lines are associated with large Faraday rotation measures, requiring that organized magnetic fields of strengths comparable to those observed in galaxies today ($\sim \mu$G) must have existed by $z \approx 1.3$, less than half of the age of the universe [7, 29, 55]. In related observations, [66] use observations of rotation measures in a large sample of quasars that extends to $z \simeq 3.7$ to show that the distribution of rotation measures broadens with redshift (despite the expected cosmological 'dilution' of high redshift rotation measures expected by the expanding universe), and that at increasing redshift progressively fewer sources are found with small rotation measures in the observer frame. The implications of this observation are that the environments of high-redshift ($z \sim 2-3$) galaxies were significantly magnetized, with the possibility that magnetic field strengths in galaxies at this epoch – a few billion years after the Big Bang – are comparable to those seen in present-day galaxies.

Beyond statistically detecting magnetic fields in high redshift galaxies, major progress has been made in mapping magnetic fields in individual cosmologically-distant galaxies. Recently, Mao et al. [72] have exploited the scenario where a background polarized source was lensed by a foreground galaxy at $z = 0.439$ to detect an axisymmetric microgauss magnetic field in the lensing galaxy as seen ~ 4.6 billion years ago. This is the highest redshift galaxy for which we have both magnetic field strength and structure information, and which can be used to test dynamo theories. In particular, this paper puts a clear upper limit of a few Gyr on the timescale for creating strong, coherent magnetic fields in galaxies!

2.2 Low-redshift galaxies

Observations of magnetic fields in nearby galaxies provide an important complement to measurements of magnetic fields in both the intergalactic medium and at high redshift. Recent work by Van Eck et al. [125] consolidates data on the properties of the magnetic fields and interstellar media of 20 local spiral galaxies, and Tabatabaei et al. [120] find that magnetic field scales with galaxy mass. All galaxies have detectable magnetic fields with ordered field strengths on the order of $1 - 10\ \mu$G, and total field strengths roughly 5 times larger, $5-50\ \mu$G, which is roughly in equipartition with the cosmic ray and kinetic energy densities (a result that has been confirmed elsewhere; [5, 74]), and which are coherent on large scales. Clear correlations exist between the total magnetic field strength and molecular gas density, as well as the star formation rate. Furthermore, the magnetic pitch angle correlates well with the mean axisymmetric magnetic field strength, but not with the local rotational shear rate. Van Eck et al. [125] also compare their results with predictions from galactic dynamo theory, and note that while some of the observations agree with these predictions, there is clear need for further theoretical work. Separately, observations of M33 (a nearby face-on spiral galaxy) show that the magnetic fields in six giant molecular cloud complexes are aligned with the spiral arms, which strongly suggests that the large-scale field in M33 anchors the molecular clouds [70]. Results such as this one will provide strong constraints on simulations that model the relationship between molecular clouds and the galaxies that contain them.

M Measurements of magnetic field properties in other types of local galaxies have been made as well. Field strengths in local elliptical galaxies are believed to be on the order of $5 - 10\ \mu$G, comparable to local spirals, although with much smaller coherence lengths – far smaller than the size of the galaxy itself [79, 135], though to date no conclusive measurement has been made. Field strengths in dwarf galaxies have been measured to have total strengths ranging from $5-15\ \mu$G and ordered fields having strengths of $1-8\ \mu$G, generally a few times weaker than local spirals, depending on the galaxy in question [15, 16, 58, 74, 83, 102]. We do note that dwarf galaxies with lower masses do tend to have lower total and ordered magnetic field strengths than larger dwarfs and spirals, and galaxies with higher star formation rates also tend to have higher magnetic field strengths (as was seen in spirals in [125]). Furthermore, it seems that, for dwarf galaxies where the structure of the magnetic field strength can be measured, the ordered component is about 20% as strong as the total magnetic field, which is comparable to much more massive local spiral galaxies.

2.3 The Milky Way

The best candidate for obfuscating the picture of magnetic fields in galaxies is our own Milky Way. The proximity to the source means that high resolution measurements can be made, but our location within the galactic disk means that comparing to other galaxies is difficult. Faraday rotation and polarization of other galaxies measures the field strength integrated through the entire thickness of the disk, while similar measurements of our own galaxy only sample fractions of the field. Further, many local radio features (such as the north polar spur and other magnetized loops and filaments) make it difficult to disentangle larger-scale magnetic field structures.

The magnetic field in the Milky Way's disk can be broken into two components: a large scale magnetic field that has a coherence length on the order of the size of the Galaxy itself, and a small scale field that is either completely random or somewhat correlated with the large scale field. Synchrotron radio emission indicates that the large scale field strength is roughly 10 μG at a Galactocentric radius of 3 kpc, and decreases to 6 μG near the Sun. This is consistent with Zeeman measurements of nearby molecular clouds (see Section 2.4). Estimates of the strength of the random magnetic field component varies from $B_{\rm rand} \gtrsim 1.3\ \mu$G [34] to 4 μG [30]. The most complete survey of dust polarization was performed by the *Planck* satellite [93], which can be seen in the right panel of Figure 1. Clearly structure can be seen on a range of scales throughout the galactic disk.

The morphology of the magnetic field in external spirals is generally parallel to spiral arms, as shown in the left panel of Figure 1. This is likely the case with the Milky Way. However, unlike other galaxies, the Milky Way seems to additionally harbor at least one reversal in the direction of the magnetic field [53, 122]. Many models exist to match the data [see the recent review by 41], including an antisymmetric spiral (similar to other galaxies), a bisymmetric spiral (which would account for reversals), a ring structure, and some superposition of these. The vertical component of the Galactic magnetic field is similarly difficult to measure. Using rotation measure from more than 1,000 extragalactic radio sources, [73] find that there is no symmetry in the vertical component at the radius of the sun, with the Galactic north field showing a field consistent with zero, and the Galactic south field of $0.31 \pm 0.03\mu$G. On the other hand, [54] find that, modeling the synchrotron intensity from WMAP, the field is consistent with an "X" shaped magnetic field. Unfortunately, none of the existing measurements are consistent with expected observations and a coherent dynamo. This is possibly due to the fact that the timescale for the coherent $\alpha - \Omega$ dynamo is longer than the age of the Galaxy, or if tidal interactions or injection of small scale magnetic fields continually disrupt the symmetry [80].

Another potentially important reservoir of magnetic field energy is in the Milky Way's circumgalactic medium (CGM), which is the huge volume of hot, diffuse baryons that exists outside of the stellar disk but within the virial radius of the dark matter halo. The CGM contains approximately half of the baryons in the entire Milky Way system [see, e.g., 92], and is considered to be important for the regulation of the star formation history of galaxies, and also responsible for controlling the bulk scaling relations seen in local galaxies [128, 129]. The CGM is metal-enriched, and thus is likely to be substantially magnetized assuming that both metals and magnetic fields originate in stars. Some evidence exists for large-scale magnetic fields in the CGM [see, e.g., Figure 7 in 39], but the detailed structure of the circumgalactic magnetic will require the Square Kilometer Array or one of its pathfinders as a probe [40].

One of the primary motivations for this study is the spatial distribution and correlations in the magnetic field, and the synchrotron and polarized dust emission that is dictated by these correlations. These are important foregrounds for studies of the polarized cosmic microwave background (CMB), and and understanding the location and structures the magnetic field produces is essential for their removal. These signals occupy different locations in the galaxy, with the polarized dust emission at relatively low galactic scale height and the synchrotron coming from higher, hotter gas. The polarized signal is best observed by converting it to two rotationally invariant quantities, E and B. The former is parity-even, while the latter is parity-odd [59, 109, 110]. The spectral amplitudes, C_ℓ^{EE} and C_ℓ^{BB} have been found that these amplitudes scale as a powerlaw in the wavenumber, ℓ^α where $\alpha = -2.4$, and has roughly twice the power in E than B [95, 96]. This is intriguingly smooth over the high-latitude sky. Preliminary studies of both galactic magnetic field [60] and driven turbulence [62] have shown promising reproduction of this signal. The proposed work will complement these works by examining the impact of the formation history and circumgalactic environment on the spatial distribution and structures in the polarized gas.

The statistical separation of the ISM and CMB signals is a necessary component of their removal. This is subject of a separate proposal that we are submitting, and beyond the scope of this one. This proposal seeks to understand the components of the signal, and provide maps for training of cleaning algorithms.

2.4 Connecting galaxies to molecular clouds

Molecular Clouds and Giant Molecular Clouds are cold (10 K) and have masses anywhere from $10^4 - 10^7$ M$_\odot$. From the limited number of Zeeman splitting measurements in cold molecular clouds, field strengths in molecular clouds range from 1 μG in low density gas ($\simeq 100$ cm^{-3}), and increase to a few mG in higher density gas ($\simeq 10^7$ cm^{-3}) [23]. Star formation is controlled by some combination of gravity, turbulence, and magnetic fields [76], and the relative importance of each is the subject of significant debate [compare, e.g., 69, 86]. The ratio of magnetic to kinetic energy is typically parameterized by the Alfvén Mach number, $\mathcal{M}_\mathrm{A} = v/v_\mathrm{A}$, where $v_\mathrm{A} = B/4\pi\sqrt{\rho}$ is the signal speed along a magnetic field line. Values of $\mathcal{M}_\mathrm{A} > 1$, so-called super-Alfvénic flow, indicates a weak magnetic field relative to kinetic energy, while $\mathcal{M}_\mathrm{A} < 1$, or sub-Alfvénic flow, indicates that magnetic fields dominate energetically. The ratio of gravitational to magnetic energy is typically parameterized by the mass-to-flux ratio, $\mu = M/\Phi$, where Φ is the magnetic flux threading a cloud of mass M, in units of the critical field strength for collapse. The actual values of $\mathcal{M}_\mathrm{A}$ and μ are difficult to measure observationally due to the challenge in measuring magnetic field strengths directly over large scales [23]. Thus, statistical and morphological arguments are made, often with different results. From measurements of column density power spectra and extinction measure

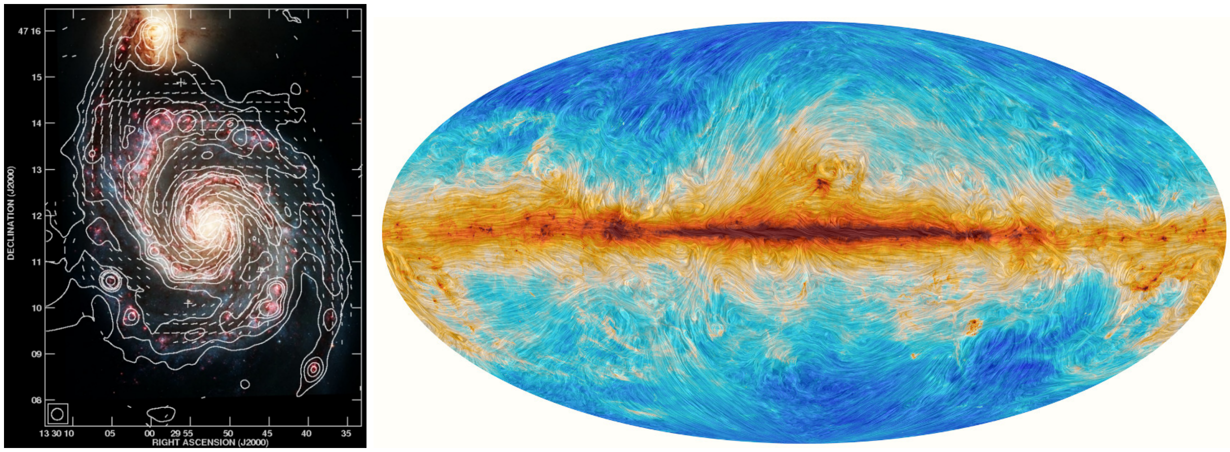

Figure 1: Coherent magnetic structure is seen in many disk galaxies. (*Left*) The magnetic field from polarized $\lambda = 3, 6$ and 20 cm radio emission (vectors) along with total emission (contours) in M51. From [33]. Optical background from *Hubble Space Telescope* (image credit: NASA, ESA, S. Beckwith (STScI) and The Hubble Heritage Team (STScI/AURA)). This shows the well-ordered nature of the magnetic field along the spiral arms. (*Right*) The *Planck* polarization map showing the 353 GHz dust intensity convolved with the direction of polarization [93]. This shows coherent structrue on a range of scales throughtout the Milky Way.

distribution in molecular clouds, [88] and [87] argue that super-Alfvénic turbulence is more consistent with molecular cloud measurements than the statistics of sub-Alfvénic models. On the other hand, [45] have shown that a difference in the slope of the velocity power spectrum between two orthogonal directions indicates that $\mathcal{M}_{\rm A} \approx 1$. Simulations [26, 65] indicate that $\mathcal{M}_{\rm A} > 1$ for clouds that formed from the warm neutral medium. Polarization measurements indicate that fields are parallel to the long axis of low mass filaments, perpendicular to the long axis of high mass filaments [68], and exhibit coherent alignment between large and small scales [67], all of which indicate $\mathcal{M}_{\rm A} < 1$. Zeeman measurements of methanol masers in star forming region indicate that the magnetic field order is imprinted on even small-scale structures over kpc scales. [36]. However, turbulence substantially impacts the structure of molecular clouds [see, e.g., 28, 71], and statistical properties indicate that turbulent kinetic energy is comparable to, if not dominant over, magnetic energy [45, 89], indicating $\mathcal{M}_{\rm A} \gtrsim 1$. Figure 2 shows the connection between molecular clouds and magnetic fields, in the left panel, in observations of field alignment with spiral structure, from Li and Henning [70], and the connection between field and the halo in a pilot study for the proposed work.

The details of the initial conditions, boundary conditions, and equation of state have profound impact on molecular cloud lifetimes and collapse rates [19, 31, 97]. Furthermore, even in models of star-forming clouds where magnetic fields play a subordinate role their effect is still non-negligible. Thus it is clear that for a detailed understanding of star formation, magnetic fields must be included. In order to capture these conditions self-consistently, **we will perform extremely high resolution simulations of isolated galaxies, extracted from cosmological initial conditions, that resolve the formation of a wide mass range of molecular clouds.**

2.5 The origin and amplification of magnetic fields in the universe

As discussed in Section 2.1, magnetic fields appear to exist everywhere in the intergalactic medium, albeit at a very low level. The physical regimes where they appear to reside – on megaparsec scales and above, and in both intergalactic filaments and in voids – argue against a galactic origin. So, then, what is the likely origin of these fields, and what theoretical constraints can we utilize?

Widrow [133, 134] provides a host of possible origins for the observed cosmological magnetic fields,

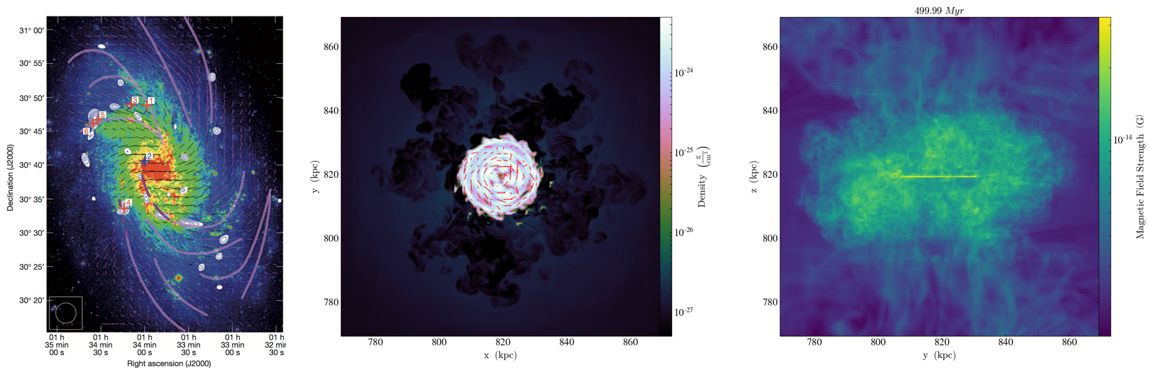

Figure 2: *(Left)*: From Li and Henning [70], magnetic fields in molecular gas (thin lines) traces spiral arms (thick lines) in M33. *(Center, Right)* From preliminary galaxy-scale simulations with an initial uniform field of 10^{-15}G a Milky Way sized galaxy produces fields up to 10^{-13}G at 20 kpc from the disk within 500 Myr. The center panel shows synthetic polarization direction following the rotational structure. The right panel shows mean magnetic field strength in an edge-on projection. This simulation has an under-resolved ISM in the galaxy, and serves as a pilot study for the proposed work.

which we briefly summarize. Magnetic fields could be generated during the inflationary epoch, during the hadronic or electroweak phase transitions, or in the radiation-dominated era prior to recombination. Depending on the nature of the effect, theoretical predictions for a minimum field strength vary hugely, from a minimum value of B $\sim 10^{-32}$ G to substantially more than a Gauss (values given at the present day). Generally speaking, theory dictates that a minimum magnetic field strength of 10^{-19} G (present-day value) and with coherence lengths on megaparsec scales must exist; the maximum theoretically-predicted value is vastly higher than the observational upper limits from the CMB of $\bar{B} \simeq 10^{-9}$ G (Section 2.1).

Given the minuscule magnetic field strengths that must have been generated prior to structure formation, and the relatively high ($> 10\ \mu$G) fields observed in both galaxies and the cores of galaxy clusters, an obvious question arises: how are such high magnetic fields generated from such weak seed fields? Straightforward adiabatic collapse of the gas (and corresponding compression of the fields) suggests an increase in magnetic field from the initial value of $\delta^{2/3}$, where δ is the ratio of maximum to original density. Given the characteristic density of the Milky Way's interstellar medium, this implies an adiabatic amplification of $\simeq 10^4 - 10^5$ times the primordial value – far too small of a value to explain the roughly 13 order of magnitude difference between the minimum inferred value in the lowest-density regions of the universe and the field strength observed in the interstellar medium.

This observation leads inexorably to the conclusion that there must be some sort of dynamo process at work that amplifies the magnetic field by using kinetic energy from the various processes associated with structure formation (i.e., gravitational collapse, rotational motion, etc.). There are two dominant modes of amplification. The *fluctuating* dynamo draws small scale turbulent energy into small scale magnetic energy. While this mechanism has growth times of 10^7 years (fast enough to generate substantial fields from extremely weak seed fields), it does not produce fields that are ordered on large scales. The second amplification mechanism is the $\alpha - \Omega$ dynamo, wherein differential rotation and buoyancy work together to add helicity to the fluid, thus amplifying the field on the large scales associated with the rotation of the galaxy. This is a slower process, which limits the large scale field available to more massive galaxies. (See [10] for a detailed review of both dynamo processes.) Either of these processes can easily magnify a seed field to the galactic field strength of 10^{-6} G [5], and compression by gravitational collapse further amplifies the galactic field strength and is responsible for the further magnification of the field to the 10^{-3} G level observed in high-density star forming regions [21]. We note that further seeds beyond the weak primordial field may be necessary to reach the observed magnetic field strengths in galaxies, particularly for the earliest galaxies – observations of strong magnetic fields at high redshift imply that dynamos have a relatively short time to operate! If that is the case, two plausible mechanisms for initial magnetic field generation are supernova remnants [133] and the jets from supermassive black holes [25, 48], both of which produce strong magnetic fields with substantial coherence lengths.

3 Proposed Work

In this project, we will use high dynamic range magnetohydrodynamical (MHD) simulations to understand how galactic-scale magnetic fields affect the formation and evolution of molecular clouds, and to identify the characteristics of these magnetized clouds that pertain to star formation. Specifically, we will use a targeted series of high resolution MHD simulations of galaxy formation, both in a cosmological context (Section 3.1.1) and as isolated, idealized galaxies (Section 3.1.2), to explore the evolution of magnetic fields through cosmic time.

Each series of simulations will use three main magnetic evolution assumptions: *dynamo-only* simulations, wherein a weak seed field fills space at the beginning of the simulation, and two *feedback* recipes that vary the amount of field injected through supernovae. These *feedback* recipes will use the toroidal injection implemented in ENZO by Butsky et al. [14]. This model deposits a fraction, σ, of supernova energy in a toroidal configuration on the grid. Our large-field run will clone [14] and use 10^{43}erg per $\mathrm{M}_{\odot}$ of initial stellar mass, and our low-field run will use 1% of that value. For each of the observational diagnostics, (Section 3.2) we will perform synthetic observations, matching noise and telescope resolution of the respective instruments, and perform Baysian estimation to compare the four populations. We expect that the *dynamo-only* simulations will fall short, which will allow us to bracket the viability of our simulations. In addition, we will perform the analysis on the unfiltered simulations in the "perfect telescope" limit, which will allow us to examine the ability of future SKA or Next Generation VLA observations to explore these regions.

These calculations will be run with the ENZO and Enzo-E codes (Section 4) using computing time secured through the XSEDE and PRAC allocation processes (Section 3.1.3). Enzo-E is the developmental exascale successor to ENZO, and will allow us to perform much larger simulations than ENZO. The majority of the production simulations in the proposed work will be suitable for either code.

3.1 Simulating the Magnetized Universe

Here we describe our target science simulations. For training and development purposes, we will run low-resolution versions of the simulations described during the first year.

3.1.1 Cosmological simulations

As described in Section 2, there is a great deal of observational evidence that magnetic fields exist in galaxies over a wide variety of masses and redshifts, and also in intergalactic space. Furthermore, it appears that the magnetic fields in star-forming galaxies build up relatively quickly, based on observations of $z \simeq 2-3$ galaxies which show that the magnetic fields measured in their interstellar medium (ISM) are roughly in equipartition with other sources of ISM energy. We will use cosmological simulations of the formation and magnetization of Milky Way-sized galaxies to explore the impact of the birth, assembly, and environment on magnetic field production.

Recently, the *Tempest* collaboration of galaxy modelers (led by collaborator O'Shea) finished two large-volume cosmological simulations using the ENZO code – one of a 25 Mpc volume, and the other 75 Mpc, both with 1024^3 root grid cells and particles, and with multiple sets of physics in each set of calculations and moderate physical resolution ($\Delta\mathrm{x} \simeq 400$ pc). One such galaxy can be seen in Figure 3 [51]. This figure shows simulations of the same galaxy, but the panel on the right has enhanced halo resolution (EHR) which substantially alters the environment of the galaxy. Taken together, these sets of calculations resolve the

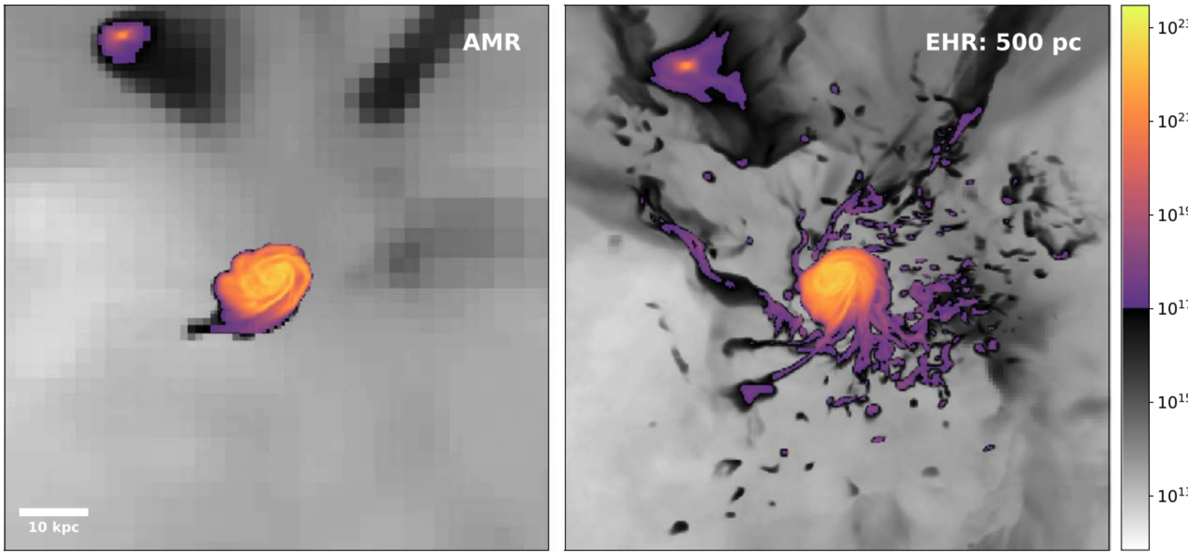

Figure 3: Two simulations using the *Tempest* suite of simulations [51]. The figure on the right has had enhanced halo resolution (EHR) which causes striking differences in the morphology of the gas around the galaxy. This will impact the evolution and structures of the magnetic field in the galaxy by altering the ability of the galaxy to expel flux.

formation of galaxies over three orders of magnitude in mass, from $\simeq 10^{10}$ to 10^{13} $M_\odot$. This encompasses galaxies ranging in size from the Small Magellenic Cloud through the largest ellipticals.

From the *Tempest* simulations, we will extract a selection of spiral galaxies of roughly Milky Way mass ($M_{gal} \simeq 1 - 2 \times 10^{12}$ $M_\odot$) that have a range of formation histories, including galaxies that have rapid early merger rates as well as those with smoother formation histories. In particular, we will include at least one galaxy with a history similar to the Milky Way, with no major mergers after $z \sim 2$. This will be our fiducial galaxy. These will be compared to observations of local spiral galaxies [e.g., 125] and to the magnetic fields in the ISM of our own Milky Way. This galaxy will be our fiducial galaxy for study, with additional galaxies of a variety of masses studied as time permits.

Once these galaxies are selected from the pilot calculations, we will re-generate the initial conditions for these galaxies at much higher mass and spatial resolution using the MUSIC cosmological IC code [37], and then re-run the calculations to the redshift of interest (typically the present day) at very high spatial resolution ($\Delta x_{min} \simeq 100$ pc) using prescriptions for metal-dependent radiative cooling, star formation and feedback, and AGN feedback, as well as magnetic field feedback. This is the state of the art for physics-rich cosmological galaxy formation simulations, and results in galaxies with reasonable $z = 0$ properties [e.g., 47, 105, 127]. We will include the equations of ideal magnetohydrodyamics using a cosmologically-motivated seed field initialized to $B \simeq 10^{-15}$ G at $z \simeq 100$ when the simulations begin.

One of the virtues of this type of cosmological simulation is that they are relatively inexpensive (see Section 3.1.3), which allows us to experiment with variations in physical models to understand the effect that model choice may have on our results. Specifically, we will experiment with the three magnetic field injection scenarios described the introduction to this section.

In addition to probing the questions posed in Sections 1 and comparing to the observations described 3.2, we will extract the galaxies at an appropriate point in their evolution and re-simulate, as describe in Section 3.1.2. This will allow us to have the most realistic initial and boundary conditions possible for the isolated simulations.

3.1.2 Galactic Simulations

While the cosmological simulations will be able to directly address a range of observationally-motivated questions about magnetic fields in galaxies, their relatively limited ($\Delta \mathrm{x} \simeq 100$ pc) spatial resolution means that they only marginally resolve larger molecular clouds, and are far too coarsely resolved to directly simulate star formation or the dynamo process. For these calculations, we will extract the target galaxies from Section 3.1.1 and embed them in isolated, non-cosmological boxes. This will allow us to increase the resolution to $\Delta \mathrm{x} \simeq 1$ pc and follow molecular cloud formation, as well as more precisely model star formation and feedback processes, albeit over substantially less than a Hubble time. Fortunately, it has been observed that Milky-way sized galaxies have magnetic field strengths by $z \sim 0.5$ that are comparable to those at the present day. This indicates that the growth time for such fields is quite short, so we will only need to simulate each galaxy for a few Gyr.

Recently, several groups have begun to explore magnetic fields in full-galaxy simulations, from cosmological initial conditions [91], in isolated, idealized disks [14, 99, 100], and also focusing on large scale structure in the IGM [126]. The proposed work will compliment these studies by bridging the lengths scales and exploring the magnetic feedback.

With these simulations, we will explore the relationship between large-scale galactic magnetization and the properties of individual molecular clouds over a wider cloud mass scale. In addition, these isolated calculations will allow us to explore in greater detail the effects that varied energy and magnetic field injection mechanisms from stellar populations (from stellar winds, AGB, and Type Ia and Type II supernovae) have on magnetic field generation, and also on the possible effect that resolution might have on dynamo amplification of magnetic fields in both spiral and elliptical galaxies [an effect that was shown to be important in high-redshift halos; 107, 119].

In these simulations we will focus the adaptive resolution on the mid-plane of the galaxy. This will allow us to and follow the injection of kinetic and magnetic energy from supernovae, and the subsequent dynamo. Each simulation will be treated with three magnetic feedback routines: the plain *dynamo-only* evolution, evolving with the field given by the cosmological simulation; and the two toroidal feedback methods. Our work will attempt to incorporate the latest knowledge in simulating the supernova driven ISM [e.g. 46, 61, 90, 111, 130] to the extent it is numerically feasible. The thermal feedback from supernovae and thermodynamics will target the formation of molecular clouds. Supernovae will be tied to star particles in order to be self-consistent, and inject $10^{51}\mathrm{erg}$ of energy and a fraction of that in toroidal magnetic energy, following [14], with the fraction depending on the simulation suite. Thermal energy will be deposited in a sphere containing 60 $\mathrm{M}_{\odot}$, following [46, 56], in order to keep the gas from radiatively cooling on an unphysically short time scale. Chemistry and thermodynamics will initially attempt to follow the description in the thorough study by [130], which simulated $\mathrm{H}^{+}, \mathrm{H}, \mathrm{H}_2, \mathrm{C}^{+}, \mathrm{CO}$. This may provide computationally prohibitive, in which case we will resort to heating and colling based on tabular interpolation computed with Cloudy [12, 32] and a density-based CO map. The chemistry is presently contained in the chemistry solver in ENZO [see, e.g., 78, 121].

3.1.3 Computing time

Zoom-in cosmological simulations of a single Milky Way-type galaxy using ENZO, with $\simeq 400$ pc resolution, require approximately 100,000 CPU-hours on TACC's Stampede resource [49, 50, 57], or slightly less on NCSA's Blue Waters. The addition of MHD roughly doubles the computational cost, and increasing the particle mass resolution by a factor of 8 (to 5×10^5 $\mathrm{M}_{\odot}$) will help to resolve early structure formation, but will increase the computational time by another factor of approximately four (rather than 8, due to judicious choices made during the creation of initial conditions that will reduce the overall number of particles). Increasing spatial resolution will result in approximately a factor of two increase in cost. Together, this suggests that a high resolution, physics-rich Milky Way-type simulation will cost roughly 100,000 node-hours on Stampede2 or Blue Waters – expensive, but not impossibly so. Isolated disk simulations will be comparably inexpensive – at most 2,500 node-hours apiece on either Stampede2 or Blue Waters. Taken together, we estimate that we will need 0.5-1 million node-hours per year on a machine like Stampede2 or Blue Waters for the cosmological and isolated disk calculations required for this proposal.

The PI Dr. Collins and collaborator have had significant success in procuring computing time on XSEDE resources as PIs and Co-PIs of numerous large allocation – they have over 25 million combined core-hours of XSEDE computing time over the past five years, most recently on XRAC allocations TG-AST090040 and AST140008. We will pursue additional computer time on XSEDE resources that will be devoted to the project described in this proposal

3.2 Observational Comparisons

We will perform synthetic observations of simulations using each of the three magnetic feedback methods described in the previous section, and will compare them to a number of recent important observations. Each comparison will use the observed data from the literature, synthetic observations employing tools previously developed by our team and previous collaborators [e.g., 3, 4, 113], convolved with resolution and noise appropriate for the target measurement. We will also employ "perfect telescope" observations directly from the data. Where possible the data reduction tools of the particular telescope will be used [e.g., CASA; 77]. This will allow us to do two things: first, we will verify the physical picture of our simulations, allowing us to isolate problems or success with the calculation; second, we will test our basic hypothesis, that magnetic feedback from supernova explosions is an essential piece of the magnetization of the universe. Finally, we will make predictions for measurements that will be made by both current and future observatories.

Our catalogue of observations will include the following: synchrotron emission polarization; thermal dust emission and its polarization; Faraday rotation measure and rotation measure synthesis; CO emission, assuming a conversion from CO-to-H_2 appropriate for the system Clark and Glover [e.g. 17], Genzel et al. [e.g. 35]; and the far-infrared (FIR) luminosity.

3.2.1 Synthetic Extragalactic Observations

We will compare our simulations to Faraday rotation measures from observations of high-redshift galaxies [2, 7, 66], the field strength, and the structure and coherence in nearby spiral galaxies [125]. We will also use measurements of large-scale intergalactic magnetic fields as a constraint [82]. Recently techniques have been developed to combine polarized synchrotron emission with Faraday Rotation depths to probe the full magnetic configuration [42, 75]. We will primarily aim to reproduce the morphology of observed integrated polarization angles of galaxies [118], the alignment of molecular clouds and spiral arms [70], and the relation between field strength and galactic properties such as mass and velocity dispersion [120, 125]. We will then make predictions for (and thus motivate) future observations of galactic magnetic field properties that will be available to the current and future radio telescopes such as the Jansky VLA, ALMA, and LOFAR, and in the further future the Square Kilometer Array pathfinder telescopes such as ASKAP, APERTIF, MeerKAT, and the SKA itself.

An extremely useful probe of the correlation of magnetic field properties and star formation is the correlation between the Far Infrared Radiation (FIR) flux and the Radio Continuum (RC). A surprisingly tight correlation between these two fluxes has been studied for several decades [44]. Both radiation sources are indirectly related to star formation, and we will aim to probe this correlation as a function of redshift. The FIR comes from re-heating of dust near sites of massive star formation, while the RC comes form synchrotron radiation [43, 84]. [81] model the radio profiles as smoothed version of the FIR profiles, indicating that for the most part the RC can be seen as a diffusive flux of cosmic rays. However, accurate measurement of this relation has not been reproduced in cosmological simulations. Modeling the FIR is done in post-production after the simulations have finished, by measuring the mass distribution in stars at a given time and using radiative transfer to measure the optical depth to FIR. Modeling the RC requires following the cosmic ray spectrum and the competition between radiation terms. These include inverse Compton scattering, ionization of neutral gas, and bremsstrahlung in addition to the synchrotron that is observable in the RC. [106] propose that at high redshift, inverse Compton may begin to dominate over synchrotron and the FIR-RC correlation will break down around $z = 2 - 4$, depending on the strength of the field and the star formation rate. Several of our simulations will include the cosmic ray treatment incorporated into Enzo and described in [103, 104], suitably modified to incorporate cosmic ray losses by the aforementioned processes. This will allow us to predict future observations by ALMA and LOFAR and to explore the utility of the RC as a probe of highly extincted star formation.

Another important correlation is the "Star Formation Main Sequence" (SFMS) of galaxies [24, 117]. This relation between star formation rate and stellar mass is a power law that is essentially constant over time, with a normalization that falls with time. This can be interpreted as a relatively quiescent, steady-state star formation process with cosmic time. Recent simulation efforts have reported good agreement with the SFMS at low redshift, but reduced star formation rate at intermediate redshifts [116]. We will measure this for not only the highly resolved galaxies, but also the entire population of galaxies formed from the cosmological simulation. This will be compared to both the low redshift behavior [11] and the high redshift properties [24]. This measurement itself is not a probe of magnetic fields, but as star formation depends on field strength we will correlate the slope and normalization of this linear relation with magnetic field strength in the constituent galaxies.

3.2.2 Synthetic Galactic Observations

One of the primary goals in this work is understanding the relationship between the large scale magnetic field of the galaxy and the magnetic fields in molecular clouds. As discussed in Section 2.4, there is clear evidence of coherent magnetic fields in galactic structure, but the importance in molecular cloud structure and dynamics is ambiguous.

The primary question is: Over what scales are the magnetic field aligned, and how does this alignment imprint on the molecular gas and impact its dynamics? To properly answer this question, we will focus on three measurements, ensuring consistency with earlier observational work and exploring field properties that have not been measured. These properties are: the properties of individual molecular clouds; the correlation between field directions at two points; and correlations between field direction and material gradients.

Molecular Cloud Properties. The mean magnetic field strength in molecular clouds is challenging to measure, but potentially of critical importance in star formation theory. We will reconcile molecular cloud properties with observational molecular clouds by comparing synthetic ^{13}CO maps with linewidth-size and mass-size relations as measured by the Galactic Ring survey [52, 101]. We will then predict the mean field strength vs. linewidth and size, and discuss the expected mass-to-flux and kinetic-to-magnetic energy distributions.

Field-Field Correlation. We will use synthetic polarization and Faraday rotation measure to measure the correlation length in the galactic scale simulations. We will also measure the distribution of alignments of magnetic fields between and within individual molecular clouds, and between each molecular cloud and the three-dimensional, kpc-scale mean field. These will be compared to the well-correlated alignment seen within molecular clouds [67] and along galactic spiral arms [33]. This will allow us to ensure the validity of the fields in our galaxies, and predict the probability of alignment between any pair of molecular clouds.

Field-Mass Correlation. We will also explore the relation between field strength and material. This has garnered recent attention as magnetic field tends to align with low density HI as seen in the GALFA-HI survey [18], and tends to lie perpendicular to higher density structure [94]. We will perform synthetic dust emission and synthetic HI maps to examine these properties. Dust polarization results will be compared to the histogram of relative orientation between polarization angle and column density gradient. For consistent comparison with the HI measurements, we will perform the Rolling Hough Transform [18] on the synthetic HI map to determine the linear structure, and correlate that with the polarization map. These measurements will assess the validity of the data. We will also explore the alignment of clouds themselves on the large scale patterns, and measure the probability of finding a cloud at a certain distance along the large scale field. This will measure the interaction of magnetic field and structure on the 100-1000 pc scale.

CMB Foregrounds We will also produce all-sky maps for the study of CMB foregrounds. Maps of the sky are necessary for training image processing and noise reduction algorithms, an essential part of the success of future missions. We will provide a suite of all-sky maps for such purposes. We will also measure the variation of C_ℓ^{EE} and C_ℓ^{BB} with time and magnetic feedback prescription. This will allow us to understand the constituent physics that sets α_{EE} and α_{BB}.

4 Tools

For this work, we will be using the adaptive mesh refinement (AMR) code ENZO, and its exascale succcessor, Enzo-E. The former is a well-established code for many computational astrophysics problems. The latter is an AMR code that has been designed for extreme scalability on both CPU and GPU architectures, but shares the same physics packages as ENZO. The use of both codes allows us to take advantage of the enormous performance gains of Enzo-E while still ensuring success of the project. As Enzo-E development is completed it will supplant ENZO for our calculations.

The ENZO code. The calculations described in this proposal will be performed using the ENZO code. ENZO is a publicly available Cartesian adaptive mesh refinement code used for the simulation of cosmological and astrophysical phenomena

ENZO [12, http://enzo-project.org]. uses a block-structured adaptive mesh refinement scheme [6] to achieve high spatial and temporal resolution, and combines an N-body adaptive particle-mesh solver for dark matter dynamics with a Piecewise Parabolic Method (PPM) hydro solver that has been extensively modified for cosmological applications and hypersonic flows [13]. In addition, the code includes a range of other physics, including both equilibrium and nonequilibrium chemistry and cooling models, radiative cooling using a Raymond-Smith model and Cloudy emissivity tables [114], and prescriptions for the formation and feedback of both stellar populations and black holes. ENZO also includes modules for magnetohydrodynamics (both the Dedner divergence-cleaning method and a constrained transport method; [22, 131, 132]) and radiation transport using a ray-casting method and flux-limited diffusion [98, 136]. ENZO has been used to model a wide variety of cosmological and astrophysical phenomena – most relevant to this proposal, ENZO has been used heavily to study high- and low-redshift cosmological structure formation [1, 27, 49, 85, 112, 114, 123, 137], the intergalactic and circumgalactic medium [38, 50, 57, 115], and the properties of star-forming molecular clouds [19–21, 63, 64, 108].

The Enzo-E code.

Enzo-E [8, 9] is the Exascale successor to ENZO. It retains the physics solvers from ENZO (e.g. the PPM and MHD solvers, chemistry, thermodynamics, star formation, etc) but replaces the AMR framework with a highly scalable "forest of oct-trees," which enables scaling AMR to hundreds of thousands of cores. Bordner and Norman [9] show Enzo-E (branded Enzo-P in that publication) scaling to 265,000 processors. This kind of scaling is not available to ENZO, and will be necessary for the future growth of computational astrophysics.

Enzo-E is currently under development under two NSF grants, #OAC 1835402 and #OAC 1835426, the latter by the collaborator, Dr. O'Shea. At present the majority of physics solvers necessary for the proposed work are present and functioning in Enzo-E. The only outstanding piece of code to be ported from ENZO to Enzo-E is the *flux correction* routines. These routines ensure conservation across refinement jumps and are necessary for accurately conserving mass and magnetic flux. The PI and collaborator have ample experience with these algorithms and foresee little difficulty in completing this development in the first year. This work should be completed by June 2020.

The YT code. Our simulations will be analyzed and visualized with the YT package [124, http://yt-project.org], which is an open source analysis and visualization toolkit for grid- and particle-based simulations.

YT was originally developed to work with ENZO, but now supports numerous simulation codes, including both grid-based and particle-based astrophysical codes (i.e., FLASH, ART, Gadget, Gasoline). Among the capabilities of YT are slices and projections (both on and off the Cartesian axes); volume renderings; halo finding and profiling; 1, 2, and 3 dimensional profiles; light-cone projections; synthetic QSO sight lines (i.e., absorption line spectra); contouring; and clump-finding. We will use YT to perform many of these analysis tasks – all of which are parallelized – and will furthermore use YT to make a variety of synthetic observations of galaxies using tools that have been developed and used by our collaboration [e.g., 3, 4]. YT can be used as a standalone code and is also callable from within an ENZO simulation, allowing analysis to be performed on in-memory datasets (a capability that will be very helpful for analysis of our larger simulations). YT is highly parallel, scales well on XSEDE computing resources, and is currently being optimized for the Stampede2 supercomputer.

5 Significance of Proposed Work

Magnetic fields are essential components of galactic structure, but the nature of their growth and morphology is elusive to understand from a theoretical and numerical standpoint. The challenge in doing so lies in the difficulty of devising a consistent treatment of initial and boundary conditions, of including the necessary physics, and in interpreting observations. The proposed project will model the origin and evolution of galactic magnetic fields, and their impact on the interstellar medium, from cosmological initial conditions to the present day. We will also create synthetic observations of synchrotron emission and dust polarization that will be invaluable for both future CMB missions and understanding existing measurements. This work will result in a deeper understanding of the evolution and morphology of magnetic fields in galaxies. This project is innovative due to its connection of cosmological structure (i.e., galaxies and their environments) down to molecular clouds and the star formation that occurs therein, and the modeling of both of these classes of objects in a unified theoretical and numerical framework. The understanding gained by doing this will be transformative in terms of our ability to more accurately model star formation through cosmic time, and will directly connect to current and future observations of magnetic fields in a range of astrophysical situations.

6 Results from prior NSF Support

Dr. David C. Collins: Dr. Collins is PI on "Magnetic Fields in the Formation of Molecular Clouds, Filaments, and Cores", (NSF AST-1616026, $298,492, 09/01/2016 - 08/31/2020) which has been examining collapse of pre-stellar cores and the role of magnetic fields therein. We have focused on 1.) the initial conditions of pre-stellar core collapse 2.) the energy budget of the collapse and rate-limiting processes and 3.) the work done on the gas by magnetic forces. **Intellectual merits:** This project is exploring the early phases of pre-stellar cores with an aim to find the earliest precursors of star forming objects. **Broader impacts:** This project involves training graduate students, and the data will be freely available upon the completion of the project. Publications are being prepared presently.

Dr. Collins was also Co-PI on an NSF Office of Advanced Cyberinfrsastructure Petascale Computing Resource Allocation grant (PRAC; ACI 1514580; "Petascale adaptive mesh simulations of Milky Way-type galaxies and their environments," $31.5K, 8/1/2015-7/31/2018) **Intellectual merits:** This project created an extensive library of simulated Milky Way-like galaxies and their environments. These will be used in the current proposal for initial conditions of the cosmological simulations. Publications: This has resulted in the publication of Hummels et al. [51].

7 Management plan and timeline

The Team.

Dr. David Collins (Co-PI) is an expert in numerical MHD methods and simulations of star forming clouds, and has participated in simulations of MHD turbulence in a variety of contexts, including first stars and galaxy clusters. He was primarily responsible for the development of the MHD solver that will be used for this work. In the proposed work, Dr. Collins will be responsible for directing the activity, analysis of simulation products, and code development as necessary.

Dr. Brian O'Shea (external collaborator, Michigan State University) is an expert in cosmological simulations of structure formation, and has modeled galaxy evolution from the earliest galaxies through present-day galaxy clusters. He is an expert on the sub-grid modeling of astrophysical processes in the ENZO code, and is wholly or partially responsible for several of ENZO's most critical modules for this project, including the star formation and feedback and AGN feedback algorithms. In this work, Dr. O'Shea and his research group at Michigan State University will be responsible for the remaining Enzo-E developments and interpretation of scientific results.

The proposal will also include one graduate student at FSU. This student will be responsible for performance of both cosmological and isolated galaxy simulations and analysis of results.

Plan and Timeline.

PI Collins will be responsible for carrying out the research described in this proposal and for reporting progress and results to the NSF, and will be responsible for overseeing the grant budget and for mentoring the graduate student.

Dr. O'Shea and the team at MSU are responsible for the final development needs of Enzo-E, and will aid in the interpretation and analysis of results.

The proposal will provide support for one unnamed graduate student. As the student has not been selected, we will structure the timeline assuming an inexperienced student.

The timetable and milestones for this project are listed below. We assume for planning purposes that the work done as a part of this project will start in August 2020. This project runs the risk of being overly ambitious. New code development brings uncertainties, and there are more interesting questions to be asked of the resulting simulations than we can possibly ask with the personnel involved. Here we describe a minimal and conservative work plan to ensure success of the primary measurements. To hedge against code errors and development setbacks, the initial phases will be run with both Enzo and Enzo-E. This will result in some additional cost as the number of simulations and their setup will increase, but the redundancy will ensure a successful results while verifying results from the new code. Once development of Enzo-E is finished, it will be used exclusively. In the unlikely event of severe delays, Enzo will be used for the production simulations.

The basic sequence of simulations for our research plan is as follows:

1. Perform a galaxy formation simulation at cosmological scales
2. Extract galactic properties from a target galaxy
3. Simulate isolated galaxy
4. Produce synthetic observations

Each of these actions uses machinery that has been well tested in ENZO and YT. Using ENZO and simple physics and low resolution (e.g. no MHD or supernovae and small enough to fit on a desktop), these actions can be done by an inexperienced graduate student in 6 months to one year. Using scientifically interesting resolution increases the simulation and analysis time substantially, as well as the time to solve problems that may arise. Similarly, including scientifically interesting physics destabilizes the code and requires more time of both the computer and the student.

The time to perform this sequence of simulations with Enzo-E is not as well determined, as many of the tools that make these simulations easy with ENZO do not exist for Enzo-E. However in principle they should have comparable time scales. The development of Enzo-E is proceeding concurrently at MSU, and should be completed June 2020.

We will spend the *first* year running a low-resolution version of this sequence for code development and training purposes. The *second* year we will begin the simulations at the target resolution with Enzo-E, as well as analyzing the magnetic history and synthetic maps. The *third* year we will further explore variations in mass, by exploring other galaxies in the Tempest simulations.

Conservatively, we will structure our work in the following way:

- **Year 1** (2020-2021): During the first year, the graduate student performs the full sequence of simulations and analysis at low resolution, with limited physics, using ENZO. We will select one of the Tempest galaxies to re-simulate with simple MHD at low resolution, extract the galactic structure at $z = 0$, re-simulate the galaxy at low resolution, and produce synthetic dust polarization maps. We will analyze magnetic field history of target galaxy. We will also begin Enzo-E on the cosmology simulations as the code becomes available. By the end of the first year we will have the complete analysis package for a single low-resolution galaxy.

  Milestones: Produce low resolution versions of both cosmology and galaxy simulations with ENZO. Analyze magnetic history and synthetic polarization maps. Begin using Enzo-E.
- **Year 2** (2021-2022): Begin a high-resolution sequence of simulations with the same target galaxy as Year 1, and all three magnetic field prescriptions. This will be done with a combination of ENZO and Enzo-E depending on the readiness of the latter. The high-resolution cosmology simulations will finish and we can analyze and publish the cosmological portion of the assembly.

  Milestones: Science-ready simulations with three magnetic prescriptions will be performed. Publication of the magnetic history of the galaxy over cosmic time. Begin the high-resolution isolated galaxy runs.
- **Year 3** (2022-2023): During the final year we will finish the galactic simulations and work on publication of the synthetic observations. We will study the magnetic assembly of the isolated galaxy, and compare to that of the cosmological simulations.

  Milestones: Finish and publish galactic simulations. Release of synthetic observations.
- **End of grant**: Public release of all new ENZO and Enzo-E modules, as well as all YT synthetic observation tools and example scripts. Public release of all simulation data and data products.

8 Intellectual merit and broader impacts

Intellectual merit: This project is novel because it will use high resolution magnetohydrodynamics simulations to self-consistently follow the evolution of plasma over a huge range of astrophysically important length, density, and temporal scales, thus bridging the gap between the cosmological structure formation that results in galactic-scale magnetic fields and the star-forming molecular clouds that form out of the magnetized interstellar medium. This is crucial because an improved understanding of how magnetized molecular clouds form within galaxies will lead to more accurate initial conditions for targeted studies of star formation, and will provide an opportunity to model that critical process in a more realistic way. The results of this project will facilitate our interpretation of observations of magnetic fields in the intergalactic medium, in both high redshift and nearby galaxies, and in the Milky Way galaxy itself.

Broader impacts: Our proposed work will have significant impact on scientists in training, who will learn to use cutting-edge numerical tools at the largest possible scale and will develop critical skills in scientific software development and data analysis. All of the tools developed as part of this work will be incorporated into widely used open-source software projects and all simulation and analysis data products will be made publicly available. This will maximize the return on this investment by enabling the community to more easily build upon this work. In addition, the result of these studies (and other astrophysics knowledge) are disseminated through "Ask a Scientist," a public outreach event we hold at Tallahassee's monthly art festival.

9 References

[1] Abel, T., G. L. Bryan, and M. L. Norman, 2002: The Formation of the First Star in the Universe. *Science*, **295**, 93–98.

[2] Athreya, R. M., V. K. Kapahi, P. J. McCarthy, and W. van Breugel, 1998: Large rotation measures in radio galaxies at Z ¿ 2. *A&A*, **329**, 809–820.

[3] Barrow, K. S. S., J. H. Wise, A. Aykutalp, B. W. O'Shea, M. L. Norman, and H. Xu, 2017: First Light II: Emission Line Extinction, Population III Stars, and X-ray Binaries. *ArXiv e-prints*.

[4] Barrow, K. S. S., J. H. Wise, M. L. Norman, B. W. O'Shea, and H. Xu, 2017: First light: exploring the spectra of high-redshift galaxies in the Renaissance Simulations. *MNRAS*, **469**, 4863–4878.

[5] Beck, R. and R. Wielebinski, 2013: *Magnetic Fields in Galaxies*. p. 641.

[6] Berger, M. J. and P. Colella, 1989: Local adaptive mesh refinement for shock hydrodynamics. *J. Comput. Phys*, **82**, 64–84.

[7] Bernet, M. L., F. Miniati, S. J. Lilly, P. P. Kronberg, and M. Dessauges-Zavadsky, 2008: Strong magnetic fields in normal galaxies at high redshift. *Nature*, **454**, 302–304.

[8] Bordner, J. and M. L. Norman, 2012: Enzo-p / cello: Scalable adaptive mesh refinement for astrophysics and cosmology. In *Proceedings of the Extreme Scaling Workshop*, University of Illinois at Urbana-Champaign, Champaign, IL, USA, BW-XSEDE '12, pp. 4:1–4:11.

[9] Bordner, J. and M. L. Norman, 2018: Computational Cosmology and Astrophysics on Adaptive Meshes using Charm++. *arXiv e-prints*, arXiv:1810.01319.

[10] Brandenburg, A. and K. Subramanian, 2005: Astrophysical magnetic fields and nonlinear dynamo theory. *Physics Reports*, **417**, 1–209.

[11] Brinchmann, J., S. Charlot, S. D. M. White, C. Tremonti, G. Kauffmann, T. Heckman, and J. Brinkmann, 2004: The physical properties of star-forming galaxies in the low-redshift Universe. *MNRAS*, **351**, 1151–1179.

[12] Bryan, G. L., M. L. Norman, B. W. O'Shea, T. Abel, J. H. Wise, M. J. Turk, D. R. Reynolds, D. C. Collins, P. Wang, S. W. Skillman, B. Smith, R. P. Harkness, J. Bordner, J.-h. Kim, M. Kuhlen, H. Xu, N. Goldbaum, C. Hummels, A. G. Kritsuk, E. Tasker, S. Skory, C. M. Simpson, O. Hahn, J. S. Oishi, G. C. So, F. Zhao, R. Cen, Y. Li, and Enzo Collaboration, 2014: ENZO: An Adaptive Mesh Refinement Code for Astrophysics. *ApJS*, **211**, 19.

[13] Bryan, G. L., M. L. Norman, J. M. Stone, R. Cen, and J. P. Ostriker, 1995: A piecewise parabolic method for cosmological hydrodynamics. *Comput. Phys. Commun.*, **89**, 149–168.

[14] Butsky, I., J. Zrake, J.-h. Kim, H.-I. Yang, and T. Abel, 2017: Ab Initio Simulations of a Supernova-driven Galactic Dynamo in an Isolated Disk Galaxy. *ApJ*, **843**, 113.

[15] Chyży, K. T., R. Beck, S. Kohle, U. Klein, and M. Urbanik, 2000: Regular magnetic fields in the dwarf irregular galaxy NGC 4449. *A&A*, **355**, 128–137.

[16] Chyży, K. T., M. Weżgowiec, R. Beck, and D. J. Bomans, 2011: Magnetic fields in Local Group dwarf irregulars. *A&A*, **529**, A94.

[17] Clark, P. C. and S. C. O. Glover, 2015: Does the CO-to-H_2 conversion factor depend on the star formation rate? *MNRAS*, **452**, 2057–2070.

[18] Clark, S. E., J. E. G. Peek, and M. E. Putman, 2014: Magnetically Aligned H I Fibers and the Rolling Hough Transform. *ApJ*, **789**, 82.

[19] Collins, D. C., A. G. Kritsuk, P. Padoan, H. Li, H. Xu, S. D. Ustyugov, and M. L. Norman, 2012: The Two States of Star-forming Clouds. *ApJ*, **750**, 13.

[20] Collins, D. C., A. G. Kritsuk, P. Padoan, M. L. Norman, and H. Xu, 2011: Power Spectra in Super Alfvenic Turbulence with Self Gravity.

[21] Collins, D. C., P. Padoan, M. L. Norman, and H. Xu, 2011: Mass and Magnetic Distributions in Self-gravitating Super-Alfvénic Turbulence with Adaptive Mesh Refinement. *ApJ*, **731**, 59.

[22] Collins, D. C., H. Xu, M. L. Norman, H. Li, and S. Li, 2010: Cosmological Adaptive Mesh Refinement Magnetohydrodynamics with Enzo. *ApJS*, **186**, 308–333.

[23] Crutcher, R. M., 2012: Magnetic Fields in Molecular Clouds. *ARA&A*, **50**, 29–63.

[24] Daddi, E., M. Dickinson, G. Morrison, R. Chary, A. Cimatti, D. Elbaz, D. Frayer, A. Renzini, A. Pope, D. M. Alexander, F. E. Bauer, M. Giavalisco, M. Huynh, J. Kurk, and M. Mignoli, 2007: Multiwavelength Study of Massive Galaxies at z˜2. I. Star Formation and Galaxy Growth. *ApJ*, **670**, 156–172.

[25] Daly, R. A. and A. Loeb, 1990: A possible origin of galactic magnetic fields. *ApJ*, **364**, 451–455.

[26] de Avillez, M. A. and D. Breitschwerdt, 2005: Global dynamical evolution of the ISM in star forming galaxies. I. High resolution 3D simulations: Effect of the magnetic field. *A&A*, **436**, 585–600.

[27] Egan, H., B. D. Smith, B. W. O'Shea, and J. M. Shull, 2014: Bringing Simulation and Observation Together to Better Understand the Intergalactic Medium. *ApJ*, **791**, 64.

[28] Elmegreen, B. G. and J. Scalo, 2004: Interstellar Turbulence I: Observations and Processes. *ARA&A*, **42**, 211–273.

[29] Farnes, J. S., S. P. O'Sullivan, M. E. Corrigan, and B. M. Gaensler, 2014: Faraday Rotation from Magnesium II Absorbers toward Polarized Background Radio Sources. *ApJ*, **795**, 63.

[30] Fauvet, L., J. F. Macías-Pérez, J. Aumont, F. X. Désert, T. R. Jaffe, A. J. Banday, M. Tristram, A. H. Waelkens, and D. Santos, 2011: Joint 3D modelling of the polarized Galactic synchrotron and thermal dust foreground diffuse emission. *A&A*, **526**, A145.

[31] Federrath, C. and R. S. Klessen, 2012: The Star Formation Rate of Turbulent Magnetized Clouds: Comparing Theory, Simulations, and Observations. *ArXiv e-prints*.

[32] Ferland, G. J., M. Chatzikos, F. Guzmán, M. L. Lykins, P. A. M. van Hoof, R. J. R. Williams, N. P. Abel, N. R. Badnell, F. P. Keenan, R. L. Porter, and P. C. Stancil, 2017: The 2017 Release Cloudy. *Revista Mexicana de Astronomia y Astrofisica*, **53**, 385–438.

[33] Fletcher, A., R. Beck, A. Shukurov, E. M. Berkhuijsen, and C. Horellou, 2011: Magnetic fields and spiral arms in the galaxy M51. *MNRAS*, **412**, 2396–2416.

[34] Gaensler, B. M., J. M. Dickey, N. M. McClure-Griffiths, A. J. Green, M. H. Wieringa, and R. F. Haynes, 2001: Radio Polarization from the Inner Galaxy at Arcminute Resolution. *ApJ*, **549**, 959–978.

[35] Genzel, R., L. J. Tacconi, F. Combes, A. Bolatto, R. Neri, A. Sternberg, M. C. Cooper, N. Bouché, F. Bournaud, A. Burkert, J. Comerford, P. Cox, M. Davis, N. M. Förster Schreiber, S. Garcia-Burillo, J. Gracia-Carpio, D. Lutz, T. Naab, S. Newman, A. Saintonge, K. Shapiro, A. Shapley, and B. Weiner, 2012: The Metallicity Dependence of the CO to H_2 Conversion Factor in z ¿= 1 Star-forming Galaxies. *ApJ*, **746**, 69.

[36] Green, J. A., N. M. McClure-Griffiths, J. L. Caswell, T. Robishaw, and L. Harvey-Smith, 2012: MAGMO: coherent magnetic fields in the star-forming regions of the Carina-Sagittarius spiral arm tangent. *MNRAS*, **425**, 2530–2547.

[37] Hahn, O. and T. Abel, 2011: Multi-scale initial conditions for cosmological simulations. *MNRAS*, **415**, 2101–2121.

[38] Hallman, E. J., B. W. O'Shea, J. O. Burns, M. L. Norman, R. Harkness, and R. Wagner, 2007: The Santa Fe Light Cone Simulation Project. I. Confusion and the Warm-Hot Intergalactic Medium in Upcoming Sunyaev-Zel'dovich Effect Surveys. *ApJ*, **671**, 27–39.

[39] Han, J. L., 2017: Observing Interstellar and Intergalactic Magnetic Fields. *ARA&A*, **55**, 111–157.

[40] Han, J. L., W. van Straten, T. J. W. Lazio, A. Deller, C. Sobey, J. Xu, D. Schnitzeler, H. Imai, S. Chatterjee, J.-P. Macquart, M. Kramer, and J. M. Cordes, 2015: Three-dimensional Tomography of the Galactic and Extragalactic Magnetoionic Medium with the SKA. *Advancing Astrophysics with the Square Kilometre Array (AASKA14)*, 41.

[41] Haverkorn, M., 2015: Magnetic Fields in the Milky Way. In Lazarian, A., E. M. de Gouveia Dal Pino, and C. Melioli, eds., *Magnetic Fields in Diffuse Media*, vol. 407 of *Astrophysics and Space Science Library*, p. 483.

[42] Heald, G., R. Braun, and R. Edmonds, 2009: The Westerbork SINGS survey. II Polarization, Faraday rotation, and magnetic fields. *A&A*, **503**, 409–435.

[43] Helou, G. and M. D. Bicay, 1993: A physical model of the infrared-to-radio correlation in galaxies. *ApJ*, **415**, 93–100.

[44] Helou, G., B. T. Soifer, and M. Rowan-Robinson, 1985: Thermal infrared and nonthermal radio - Remarkable correlation in disks of galaxies. *ApJL*, **298**, L7–L11.

[45] Heyer, M. H. and C. M. Brunt, 2012: Trans-Alfvénic motions in the Taurus molecular cloud. *MNRAS*, **420**, 1562–1569.

[46] Hill, A. S., M. R. Joung, M.-M. Mac Low, R. A. Benjamin, L. M. Haffner, C. Klingenberg, and K. Waagan, 2012: Vertical Structure of a Supernova-driven Turbulent, Magnetized Interstellar Medium. *ApJ*, **750**, 104.

[47] Hopkins, P. F., D. Kereš, J. Oñorbe, C.-A. Faucher-Giguère, E. Quataert, N. Murray, and J. S. Bullock, 2014: Galaxies on FIRE (Feedback In Realistic Environments): stellar feedback explains cosmologically inefficient star formation. *MNRAS*, **445**, 581–603.

[48] Hoyle, F., 1969: Magnetic Fields and Highly Condensed Objects. *Nature*, **223**, 936.

[49] Hummels, C. B. and G. L. Bryan, 2012: Adaptive Mesh Refinement Simulations of Galaxy Formation: Exploring Numerical and Physical Parameters. *ApJ*, **749**, 140.

[50] Hummels, C. B., G. L. Bryan, B. D. Smith, and M. J. Turk, 2013: Constraints on hydrodynamical subgrid models from quasar absorption line studies of the simulated circumgalactic medium. *MNRAS*, **430**, 1548–1565.

[51] Hummels, C. B., B. D. Smith, P. F. Hopkins, B. W. O'Shea, D. W. Silvia, J. K. Werk, N. Lehner, J. H. Wise, D. C. Collins, and I. S. Butsky, 2019: The Impact of Enhanced Halo Resolution on the Simulated Circumgalactic Medium. *ApJ*, **882(2)**, 156.

[52] Jackson, J. M., J. M. Rathborne, R. Y. Shah, R. Simon, T. M. Bania, D. P. Clemens, E. T. Chambers, A. M. Johnson, M. Dormody, R. Lavoie, and M. H. Heyer, 2006: The Boston University-Five College Radio Astronomy Observatory Galactic Ring Survey. *ApJS*, **163**, 145–159.

[53] Jaffe, T. R., A. J. Banday, J. P. Leahy, S. Leach, and A. W. Strong, 2011: Connecting synchrotron, cosmic rays and magnetic fields in the plane of the Galaxy. *MNRAS*, **416**, 1152–1162.

[54] Jansson, R. and G. R. Farrar, 2012: The Galactic Magnetic Field. *ApJL*, **761**, L11.

[55] Joshi, R. and H. Chand, 2013: Dependence of residual rotation measure on intervening Mg II absorbers at cosmic distances. *MNRAS*, **434**, 3566–3571.

[56] Joung, M. K. R. and M.-M. Mac Low, 2006: Turbulent Structure of a Stratified Supernova-driven Interstellar Medium. *ApJ*, **653**, 1266–1279.

[57] Joung, M. R., M. E. Putman, G. L. Bryan, X. Fernández, and J. E. G. Peek, 2012: Gas Accretion is Dominated by Warm Ionized Gas in Milky Way Mass Galaxies at z ˜ 0. *ApJ*, **759**, 137.

[58] Jurusik, W., R. T. Drzazga, M. Jableka, K. T. Chyży, R. Beck, U. Klein, and M. Weżgowiec, 2014: Magnetic fields and star formation in low-mass Magellanic-type and peculiar galaxies. *A&A*, **567**, A134.

[59] Kamionkowski, M., A. Kosowsky, and A. Stebbins, 1997: A Probe of Primordial Gravity Waves and Vorticity. *Physical Review Letters*, **78(11)**, 2058–2061.

[60] Kim, C.-G., S. K. Choi, and R. Flauger, 2019: Dust Polarization Maps from TIGRESS: E/B power asymmetry and TE correlation. *arXiv e-prints*, arXiv:1901.07079.

[61] Kim, C.-G. and E. C. Ostriker, 2015: Momentum Injection by Supernovae in the Interstellar Medium. *ApJ*, **802**, 99.

[62] Kritsuk, A. G., R. Flauger, and S. D. Ustyugov, 2018: Dust-Polarization Maps for Local Interstellar Turbulence. *Physical Review Letters*, **121(2)**, 021104.

[63] Kritsuk, A. G., Å. Nordlund, D. Collins, P. Padoan, M. L. Norman, T. Abel, R. Banerjee, C. Federrath, M. Flock, D. Lee, P. S. Li, W.-C. Müller, R. Teyssier, S. D. Ustyugov, C. Vogel, and H. Xu, 2011: Comparing Numerical Methods for Isothermal Magnetized Supersonic Turbulence. *ApJ*, **737**, 13.

[64] Kritsuk, A. G., M. L. Norman, and R. Wagner, 2011: On the Density Distribution in Star-forming Interstellar Clouds. *ApJL*, **727**, L20.

[65] Kritsuk, A. G., S. D. Ustyugov, and M. L. Norman, 2011: Interstellar Turbulence and Star Formation. In J. Alves, B. G. Elmegreen, J. M. Girart, & V. Trimble, ed., *Computational Star Formation*, vol. 270 of *IAU Symposium*, pp. 179–186.

[66] Kronberg, P. P., M. L. Bernet, F. Miniati, S. J. Lilly, M. B. Short, and D. M. Higdon, 2008: A Global Probe of Cosmic Magnetic Fields to High Redshifts. *ApJ*, **676**, 70–79.

[67] Li, H.-b., C. D. Dowell, A. Goodman, R. Hildebrand, and G. Novak, 2009: Anchoring Magnetic Field in Turbulent Molecular Clouds. *ApJ*, **704**, 891–897.

[68] Li, H.-b., M. Fang, T. Henning, and J. Kainulainen, 2013: The link between magnetic fields and filamentary clouds: bimodal cloud orientations in the Gould Belt. *MNRAS*, **436**, 3707–3719.

[69] Li, H.-b., A. Goodman, T. K. Sridharan, M. Houde, Z.-Y. Li, G. Novak, and K. S. Tang, 2014: The Link between Magnetic Fields and Cloud/Star Formation. *ArXiv e-prints*.

[70] Li, H.-B. and T. Henning, 2011: The alignment of molecular cloud magnetic fields with the spiral arms in M33. *Nature*, **479**, 499–501.

[71] Mac Low, M.-M. and R. S. Klessen, 2004: Control of star formation by supersonic turbulence. *Rev. Mod. Phys.* , **76**, 125–194.

[72] Mao, S. A., C. Carilli, B. M. Gaensler, O. Wucknitz, C. Keeton, A. Basu, R. Beck, P. P. Kronberg, and E. Zweibel, 2017: Detection of microgauss coherent magnetic fields in a galaxy five billion years ago. *Nature Astronomy*, **1**, 621–626.

[73] Mao, S. A., B. M. Gaensler, M. Haverkorn, E. G. Zweibel, G. J. Madsen, N. M. McClure-Griffiths, A. Shukurov, and P. P. Kronberg, 2010: A Survey of Extragalactic Faraday Rotation at High Galactic Latitude: The Vertical Magnetic Field of the Milky Way Toward the Galactic Poles. *ApJ*, **714**, 1170–1186.

[74] Mao, S. A., N. M. McClure-Griffiths, B. M. Gaensler, M. Haverkorn, R. Beck, D. McConnell, M. Wolleben, S. Stanimirović, J. M. Dickey, and L. Staveley-Smith, 2012: Magnetic Field Structure of the Large Magellanic Cloud from Faraday Rotation Measures of Diffuse Polarized Emission. *ApJ*, **759**, 25.

[75] Mao, S. A., E. Zweibel, A. Fletcher, J. Ott, and F. Tabatabaei, 2015: Properties of the Magneto-ionic Medium in the Halo of M51 Revealed by Wide-band Polarimetry. *ApJ*, **800**, 92.

[76] McKee, C. F. and E. C. Ostriker, 2007: Theory of Star Formation. *ARA&A*, **45**, 565–687.

[77] McMullin, J. P., B. Waters, D. Schiebel, W. Young, and K. Golap, 2007: CASA Architecture and Applications. In Shaw, R. A., F. Hill, and D. J. Bell, eds., *Astronomical Data Analysis Software and Systems XVI*, vol. 376 of *Astronomical Society of the Pacific Conference Series*, p. 127.

[78] Meece, G. R., B. D. Smith, and B. W. O'Shea, 2014: Fragmentation in Dusty Low-metallicity Star-forming Halos. *ApJ*, **783**, 75.

[79] Moss, D. and A. Shukurov, 1996: Turbulence and magnetic fields in elliptical galaxies. *MNRAS*, **279**, 229–239.

[80] Moss, D., R. Stepanov, T. G. Arshakian, R. Beck, M. Krause, and D. Sokoloff, 2012: Multiscale magnetic fields in spiral galaxies: evolution and reversals. *A&A*, **537**, A68.

[81] Murphy, E. J., G. Helou, R. Braun, J. D. P. Kenney, L. Armus, D. Calzetti, B. T. Draine, R. C. Kennicutt, Jr., H. Roussel, F. Walter, G. J. Bendo, B. Buckalew, D. A. Dale, C. W. Engelbracht, J. D. T. Smith, and M. D. Thornley, 2006: The Effect of Star Formation on the Far-Infrared-Radio Correlation within Galaxies. *ApJL*, **651**, L111–L115.

[82] Neronov, A. and I. Vovk, 2010: Evidence for Strong Extragalactic Magnetic Fields from Fermi Observations of TeV Blazars. *Science*, **328**, 73–.

[83] Nikiel-Wroczyński, B., M. Soida, M. Urbanik, R. Beck, and D. J. Bomans, 2013: Intergalactic magnetic fields in Stephan's Quintet. *MNRAS*, **435**, 149–157.

[84] Niklas, S. and R. Beck, 1997: A new approach to the radio-far infrared correlation for non-calorimeter galaxies. *A&A*, **320**, 54–64.

[85] O'Shea, B. W. and M. L. Norman, 2007: Population III Star Formation in a ΛCDM Universe. I. The Effect of Formation Redshift and Environment on Protostellar Accretion Rate. *ApJ*, **654**, 66–92.

[86] Padoan, P., C. Federrath, G. Chabrier, N. J. Evans, II, D. Johnstone, J. K. Jørgensen, C. F. McKee, and Å. Nordlund, 2013: The Star Formation Rate of Molecular Clouds. *ArXiv e-prints*.

[87] Padoan, P., R. Jimenez, M. Juvela, and Å. Nordlund, 2004: The Average Magnetic Field Strength in Molecular Clouds: New Evidence of Super-Alfvénic Turbulence. *ApJL*, **604**, L49–L52.

[88] Padoan, P. and Å. Nordlund, 1999: A Super-Alfvénic Model of Dark Clouds. *ApJ*, **526**, 279–294.

[89] —, 2004: The "Mysterious" Origin of Brown Dwarfs. *ApJ*, **617**, 559–564.

[90] Padoan, P., L. Pan, T. Haugbølle, and Å. Nordlund, 2016: Supernova Driving. I. The Origin of Molecular Cloud Turbulence. *ApJ*, **822**, 11.

[91] Pakmor, R., F. A. Gomez, R. J. J. Grand, F. Marinacci, C. M. Simpson, V. Springel, D. J. R. Campbell, C. S. Frenk, T. Guillet, C. Pfrommer, and S. D. M. White, 2017: Magnetic field formation in the Milky Way-like disk galaxies of the Auriga project. *ArXiv e-prints*.

[92] Peeples, M. S., J. K. Werk, J. Tumlinson, B. D. Oppenheimer, J. X. Prochaska, N. Katz, and D. H. Weinberg, 2014: A Budget and Accounting of Metals at z ˜ 0: Results from the COS-Halos Survey. *ApJ*, **786**, 54.

[93] Planck Collaboration, R. Adam, P. A. R. Ade, N. Aghanim, M. I. R. Alves, M. Arnaud, D. Arzoumanian, M. Ashdown, J. Aumont, C. Baccigalupi, A. J. Banday, R. B. Barreiro, N. Bartolo, E. Battaner, K. Benabed, A. Benoit-Lévy, J.-P. Bernard, M. Bersanelli, P. Bielewicz, A. Bonaldi, L. Bonavera, J. R. Bond, J. Borrill, F. R. Bouchet, F. Boulanger, A. Bracco, C. Burigana, R. C. Butler, E. Calabrese, J.-F. Cardoso, A. Catalano, A. Chamballu, H. C. Chiang, P. R. Christensen, S. Colombi, L. P. L. Colombo, C. Combet, F. Couchot, B. P. Crill, A. Curto, F. Cuttaia, L. Danese, R. D. Davies, R. J. Davis, P. de Bernardis, A. de Rosa, G. de Zotti, J. Delabrouille, C. Dickinson, J. M. Diego, H. Dole, S. Donzelli, O. Doré, M. Douspis, A. Ducout, X. Dupac, G. Efstathiou, F. Elsner, T. A. Enßlin, H. K. Eriksen, E. Falgarone, K. Ferrière, F. Finelli, O. Forni, M. Frailis, A. A. Fraisse, E. Franceschi, A. Frejsel, S. Galeotta, S. Galli, K. Ganga, T. Ghosh, M. Giard, E. Gjerløw, J. González-Nuevo, K. M. Górski, A. Gregorio, A. Gruppuso, V. Guillet, F. K. Hansen, D. Hanson, D. L. Harrison, S. Henrot-Versillé, C. Hernández-Monteagudo, D. Herranz, S. R. Hildebrandt, E. Hivon, W. A. Holmes, W. Hovest, K. M. Huffenberger, G. Hurier, A. H. Jaffe, T. R. Jaffe, W. C. Jones, E. Keihänen, R. Keskitalo, T. S. Kisner, R. Kneissl, J. Knoche, M. Kunz, H. Kurki-Suonio,

G. Lagache, J.-M. Lamarre, A. Lasenby, M. Lattanzi, R. Leonardi, F. Levrier, M. Liguori, P. B. Lilje, M. Linden-Vørnle, M. López-Caniego, P. M. Lubin, J. F. Macías-Pérez, B. Maffei, D. Maino, N. Mandolesi, M. Maris, D. J. Marshall, P. G. Martin, E. Martínez-González, S. Masi, S. Matarrese, P. Mazzotta, A. Melchiorri, L. Mendes, A. Mennella, M. Migliaccio, M.-A. Miville-Deschênes, A. Moneti, L. Montier, G. Morgante, D. Mortlock, D. Munshi, J. A. Murphy, P. Naselsky, P. Natoli, H. U. Nørgaard-Nielsen, F. Noviello, D. Novikov, I. Novikov, N. Oppermann, C. A. Oxborrow, L. Pagano, F. Pajot, D. Paoletti, F. Pasian, O. Perdereau, L. Perotto, F. Perrotta, V. Pettorino, F. Piacentini, M. Piat, S. Plaszczynski, E. Pointecouteau, G. Polenta, N. Ponthieu, L. Popa, G. W. Pratt, S. Prunet, J.-L. Puget, J. P. Rachen, W. T. Reach, M. Reinecke, M. Remazeilles, C. Renault, I. Ristorcelli, G. Rocha, G. Roudier, J. A. Rubiño-Martín, B. Rusholme, M. Sandri, D. Santos, G. Savini, D. Scott, J. D. Soler, L. D. Spencer, V. Stolyarov, R. Sudiwala, R. Sunyaev, D. Sutton, A.-S. Suur-Uski, J.-F. Sygnet, J. A. Tauber, L. Terenzi, L. Toffolatti, M. Tomasi, M. Tristram, M. Tucci, G. Umana, L. Valenziano, J. Valiviita, B. Van Tent, P. Vielva, F. Villa, L. A. Wade, B. D. Wandelt, I. K. Wehus, H. Wiesemeyer, D. Yvon, A. Zacchei, and A. Zonca, 2015: Planck intermediate results. XIX. An overview of the polarized thermal emission from Galactic dust. *A&A*, **576**, A104.

[94] Planck Collaboration, R. Adam, P. A. R. Ade, N. Aghanim, M. I. R. Alves, M. Arnaud, D. Arzoumanian, M. Ashdown, J. Aumont, C. Baccigalupi, A. J. Banday, R. B. Barreiro, N. Bartolo, E. Battaner, K. Benabed, A. Benoit-Lévy, J.-P. Bernard, M. Bersanelli, P. Bielewicz, A. Bonaldi, L. Bonavera, J. R. Bond, J. Borrill, F. R. Bouchet, F. Boulanger, A. Bracco, C. Burigana, R. C. Butler, E. Calabrese, J.-F. Cardoso, A. Catalano, A. Chamballu, H. C. Chiang, P. R. Christensen, S. Colombi, L. P. L. Colombo, C. Combet, F. Couchot, B. P. Crill, A. Curto, F. Cuttaia, L. Danese, R. D. Davies, R. J. Davis, P. de Bernardis, A. de Rosa, G. de Zotti, J. Delabrouille, C. Dickinson, J. M. Diego, H. Dole, S. Donzelli, O. Doré, M. Douspis, A. Ducout, X. Dupac, G. Efstathiou, F. Elsner, T. A. Enßlin, H. K. Eriksen, E. Falgarone, K. Ferrière, F. Finelli, O. Forni, M. Frailis, A. A. Fraisse, E. Franceschi, A. Frejsel, S. Galeotta, S. Galli, K. Ganga, T. Ghosh, M. Giard, E. Gjerløw, J. González-Nuevo, K. M. Górski, A. Gregorio, A. Gruppuso, V. Guillet, F. K. Hansen, D. Hanson, D. L. Harrison, S. Henrot-Versillé, C. Hernández-Monteagudo, D. Herranz, S. R. Hildebrandt, E. Hivon, W. A. Holmes, W. Hovest, K. M. Huffenberger, G. Hurier, A. H. Jaffe, T. R. Jaffe, W. C. Jones, E. Keihänen, R. Keskitalo, T. S. Kisner, R. Kneissl, J. Knoche, M. Kunz, H. Kurki-Suonio, G. Lagache, J.-M. Lamarre, A. Lasenby, M. Lattanzi, C. R. Lawrence, R. Leonardi, F. Levrier, M. Liguori, P. B. Lilje, M. Linden-Vørnle, M. López-Caniego, P. M. Lubin, J. F. Macías-Pérez, B. Maffei, D. Maino, N. Mandolesi, M. Maris, D. J. Marshall, P. G. Martin, E. Martínez-González, S. Masi, S. Matarrese, P. Mazzotta, A. Melchiorri, L. Mendes, A. Mennella, M. Migliaccio, M.-A. Miville-Deschênes, A. Moneti, L. Montier, G. Morgante, D. Mortlock, D. Munshi, J. A. Murphy, P. Naselsky, P. Natoli, H. U. Nørgaard-Nielsen, F. Noviello, D. Novikov, I. Novikov, N. Oppermann, C. A. Oxborrow, L. Pagano, F. Pajot, D. Paoletti, F. Pasian, O. Perdereau, L. Perotto, F. Perrotta, V. Pettorino, F. Piacentini, M. Piat, S. Plaszczynski, E. Pointecouteau, G. Polenta, N. Ponthieu, L. Popa, G. W. Pratt, S. Prunet, J.-L. Puget, J. P. Rachen, W. T. Reach, M. Reinecke, M. Remazeilles, C. Renault, I. Ristorcelli, G. Rocha, G. Roudier, J. A. Rubiño-Martín, B. Rusholme, M. Sandri, D. Santos, G. Savini, D. Scott, J. D. Soler, L. D. Spencer, V. Stolyarov, R. Sudiwala, R. Sunyaev, D. Sutton, A.-S. Suur-Uski, J.-F. Sygnet, J. A. Tauber, L. Terenzi, L. Toffolatti, M. Tomasi, M. Tristram, M. Tucci, G. Umana, L. Valenziano, J. Valiviita, B. Van Tent, P. Vielva, F. Villa, L. A. Wade, B. D. Wandelt, I. K. Wehus, H. Wiesemeyer, D. Yvon, A. Zacchei, and A. Zonca, 2014: Planck intermediate results. XXXII. The relative orientation between the magnetic field and structures traced by interstellar dust. *ArXiv e-prints*.

[95] Planck Collaboration, P. A. R. Ade, N. Aghanim, M. Arnaud, M. Ashdown, J. Aumont, C. Bac-

cigalupi, A. J. Banday, R. B. Barreiro, N. Bartolo, E. Battaner, K. Benabed, A. Benoit-Lévy, J. P. Bernard, M. Bersanelli, P. Bielewicz, A. Bonaldi, L. Bonavera, J. R. Bond, J. Borrill, F. R. Bouchet, F. Boulanger, A. Bracco, C. Burigana, E. Calabrese, J. F. Cardoso, A. Catalano, A. Chamballu, R. R. Chary, H. C. Chiang, P. R. Christensen, L. P. L. Colombo, C. Combet, B. P. Crill, A. Curto, F. Cuttaia, L. Danese, R. D. Davies, R. J. Davis, P. de Bernardis, A. de Rosa, G. de Zotti, J. Delabrouille, J. M. Delouis, C. Dickinson, J. M. Diego, H. Dole, S. Donzelli, O. Doré, M. Douspis, J. Dunkley, X. Dupac, G. Efstathiou, F. Elsner, T. A. Enßlin, H. K. Eriksen, E. Falgarone, K. Ferrière, F. Finelli, O. Forni, M. Frailis, A. A. Fraisse, E. Franceschi, A. Frolov, S. Galeotta, S. Galli, K. Ganga, T. Ghosh, M. Giard, E. Gjerløw, J. González-Nuevo, K. M. Górski, A. Gruppuso, V. Guillet, F. K. Hansen, D. L. Harrison, G. Helou, C. Hernández-Monteagudo, D. Herranz, S. R. Hildebrandt, E. Hivon, A. Hornstrup, W. Hovest, Z. Huang, K. M. Huffenberger, G. Hurier, T. R. Jaffe, W. C. Jones, M. Juvela, E. Keihänen, R. Keskitalo, T. S. Kisner, R. Kneissl, J. Knoche, M. Kunz, H. Kurki-Suonio, J. M. Lamarre, A. Lasenby, M. Lattanzi, C. R. Lawrence, R. Leonardi, J. León-Tavares, F. Levrier, M. Liguori, P. B. Lilje, M. Linden-Vørnle, M. López- Caniego, P. M. Lubin, J. F. Macías-Pérez, B. Maffei, D. Maino, N. Mandolesi, M. Maris, P. G. Martin, E. Martínez- González, S. Masi, S. Matarrese, P. McGehee, A. Melchiorri, A. Mennella, M. Migliaccio, M. A. Miville-Deschênes, A. Moneti, L. Montier, G. Morgante, D. Mortlock, D. Munshi, J. A. Murphy, P. Naselsky, F. Nati, P. Natoli, D. Novikov, I. Novikov, N. Oppermann, C. A. Oxborrow, L. Pagano, F. Pajot, D. Paoletti, F. Pasian, O. Perdereau, V. Pettorino, F. Piacentini, M. Piat, E. Pierpaoli, S. Plaszczynski, E. Pointecouteau, G. Polenta, N. Ponthieu, G. W. Pratt, S. Prunet, J. L. Puget, J. P. Rachen, W. T. Reach, R. Rebolo, M. Reinecke, M. Remazeilles, C. Renault, A. Renzi, I. Ristorcelli, G. Rocha, C. Rosset, M. Rossetti, G. Roudier, J. A. Rubiño-Martín, B. Rusholme, M. Sandri, D. Santos, M. Savelainen, G. Savini, D. Scott, P. Serra, J. D. Soler, V. Stolyarov, R. Sudiwala, R. Sunyaev, A. S. Suur-Uski, J. F. Sygnet, J. A. Tauber, L. Terenzi, L. Toffolatti, M. Tomasi, M. Tristram, M. Tucci, G. Umana, L. Valenziano, J. Valiviita, B. Van Tent, P. Vielva, F. Villa, L. A. Wade, B. D. Wandelt, I. K. Wehus, D. Yvon, A. Zacchei, and A. Zonca, 2016: Planck intermediate results. XXXVIII. E- and B-modes of dust polarization from the magnetized filamentary structure of the interstellar medium. *A&A*, **586**, A141.

[96] Planck Collaboration, Y. Akrami, M. Ashdown, J. Aumont, C. Baccigalupi, M. Ballardini, A. J. Banday, R. B. Barreiro, N. Bartolo, S. Basak, K. Benabed, J.-P. Bernard, M. Bersanelli, P. Bielewicz, J. R. Bond, J. Borrill, F. R. Bouchet, F. Boulanger, A. Bracco, M. Bucher, C. Burigana, E. Calabrese, J.-F. Cardoso, J. Carron, H. C. Chiang, C. Combet, B. P. Crill, P. de Bernardis, G. de Zotti, J. Delabrouille, J.-M. Delouis, E. Di Valentino, C. Dickinson, J. M. Diego, A. Ducout, X. Dupac, F. Elsner, T. A. Enßlin, E. Falgarone, Y. Fantaye, K. Ferrière, F. Finelli, F. Forastieri, M. Frailis, A. A. Fraisse, E. Franceschi, A. Frolov, S. Galeotta, S. Galli, K. Ganga, R. T. Génova-Santos, T. Ghosh, J. González-Nuevo, K. M. Górski, A. Gruppuso, J. E. Gudmundsson, V. Guillet, W. Handley, F. K. Hansen, D. Herranz, Z. Huang, A. H. Jaffe, W. C. Jones, E. Keihänen, R. Keskitalo, K. Kiiveri, J. Kim, N. Krachmalnicoff, M. Kunz, H. Kurki-Suonio, J.-M. Lamarre, A. Lasenby, M. Le Jeune, F. Levrier, M. Liguori, P. B. Lilje, V. Lindholm, M. López-Caniego, P. M. Lubin, Y.-Z. Ma, J. F. Macías-Pérez, G. Maggio, D. Maino, N. Mandolesi, A. Mangilli, P. G. Martin, E. Martínez-González, S. Matarrese, J. D. McEwen, P. R. Meinhold, A. Melchiorri, M. Migliaccio, M.-A. Miville-Deschênes, D. Molinari, A. Moneti, L. Montier, G. Morgante, P. Natoli, L. Pagano, D. Paoletti, V. Pettorino, F. Piacentini, G. Polenta, J. P. Rachen, M. Reinecke, M. Remazeilles, A. Renzi, G. Rocha, C. Rosset, G. Roudier, J. A. Rubiño-Martín, B. Ruiz-Granados, L. Salvati, M. Sandri, M. Savelainen, D. Scott, J. D. Soler, L. D. Spencer, J. A. Tauber, D. Tavagnacco, L. Toffolatti, M. Tomasi, T. Trombetti, J. Valiviita, F. Vansyngel, F. Van Tent, P. Vielva, F. Villa, N. Vittorio, I. K. Wehus, A. Zacchei, and A. Zonca, 2018: Planck intermediate results. LIV. Polarized dust foregrounds. *ArXiv e-prints*.

[97] Rey-Raposo, R., C. Dobbs, and A. Duarte-Cabral, 2014: Are turbulent spheres suitable initial conditions for star-forming clouds? *ArXiv e-prints*.

[98] Reynolds, D. R., J. C. Hayes, P. Paschos, and M. L. Norman, 2009: Self-consistent solution of cosmological radiation-hydrodynamics and chemical ionization. *J. Comput. Phys*, **228**, 6833–6854.

[99] Rieder, M. and R. Teyssier, 2016: A small-scale dynamo in feedback-dominated galaxies as the origin of cosmic magnetic fields - I. The kinematic phase. *MNRAS*, **457**, 1722–1738.

[100] —, 2017: A small-scale dynamo in feedback-dominated galaxies - II. The saturation phase and the final magnetic configuration. *MNRAS*, **471**, 2674–2686.

[101] Roman-Duval, J., J. M. Jackson, M. Heyer, J. Rathborne, and R. Simon, 2010: Physical Properties and Galactic Distribution of Molecular Clouds Identified in the Galactic Ring Survey. *ApJ*, **723**, 492–507.

[102] Roychowdhury, S. and J. N. Chengalur, 2012: The radio-far-infrared correlation in the faintest star-forming dwarf galaxies. *MNRAS*, **423**, L127–L131.

[103] Salem, M. and G. L. Bryan, 2014: Cosmic ray driven outflows in global galaxy disc models. *MNRAS*, **437**, 3312–3330.

[104] Salem, M., G. L. Bryan, and C. Hummels, 2014: Cosmological Simulations of Galaxy Formation with Cosmic Rays. *ApJL*, **797**, L18.

[105] Scannapieco, C., M. Wadepuhl, O. H. Parry, J. F. Navarro, A. Jenkins, V. Springel, R. Teyssier, E. Carlson, H. M. P. Couchman, R. A. Crain, C. Dalla Vecchia, C. S. Frenk, C. Kobayashi, P. Monaco, G. Murante, T. Okamoto, T. Quinn, J. Schaye, G. S. Stinson, T. Theuns, J. Wadsley, S. D. M. White, and R. Woods, 2012: The Aquila comparison project: the effects of feedback and numerical methods on simulations of galaxy formation. *MNRAS*, **423**, 1726–1749.

[106] Schleicher, D. R. G. and R. Beck, 2013: A new interpretation of the far-infrared - radio correlation and the expected breakdown at high redshift. *A&A*, **556**, A142.

[107] Schleicher, D. R. G., M. Latif, J. Schober, W. Schmidt, S. Bovino, C. Federrath, J. Niemeyer, R. Banerjee, and R. S. Klessen, 2013: Magnetic fields during high redshift structure formation. *Astronomische Nachrichten*, **334**, 531.

[108] Schmidt, W., D. C. Collins, and A. G. Kritsuk, 2013: Local support against gravity in magnetoturbulent fluids. *MNRAS*, **431**, 3196–3215.

[109] Seljak, U., 1997: Measuring Polarization in the Cosmic Microwave Background. *ApJ*, **482(1)**, 6–16.

[110] Seljak, U. and M. Zaldarriaga, 1997: Signature of Gravity Waves in the Polarization of the Microwave Background. *Physical Review Letters*, **78(11)**, 2054–2057.

[111] Shetty, R. and E. C. Ostriker, 2012: Maximally Star-forming Galactic Disks. II. Vertically Resolved Hydrodynamic Simulations of Starburst Regulation. *ApJ*, **754**, 2.

[112] Simpson, C. M., G. L. Bryan, K. V. Johnston, B. D. Smith, M.-M. Mac Low, S. Sharma, and J. Tumlinson, 2013: The effect of feedback and reionization on star formation in low-mass dwarf galaxy haloes. *MNRAS*, **432**, 1989–2011.

[113] Skillman, S. W., H. Xu, E. J. Hallman, B. W. O'Shea, J. O. Burns, H. Li, D. C. Collins, and M. L. Norman, 2013: Cosmological Magnetohydrodynamic Simulations of Galaxy Cluster Radio Relics: Insights and Warnings for Observations. *ApJ*, **765**, 21.

[114] Smith, B., S. Sigurdsson, and T. Abel, 2008: Metal cooling in simulations of cosmic structure formation. *MNRAS*, **385**, 1443–1454.

[115] Smith, B. D., E. J. Hallman, J. M. Shull, and B. W. O'Shea, 2011: The Nature of the Warm/Hot Intergalactic Medium. I. Numerical Methods, Convergence, and O VI Absorption. *ApJ*, **731**, 6–+.

[116] Sparre, M., C. C. Hayward, V. Springel, M. Vogelsberger, S. Genel, P. Torrey, D. Nelson, D. Sijacki, and L. Hernquist, 2015: The star formation main sequence and stellar mass assembly of galaxies in the Illustris simulation. *MNRAS*, **447**, 3548–3563.

[117] Speagle, J. S., C. L. Steinhardt, P. L. Capak, and J. D. Silverman, 2014: A Highly Consistent Framework for the Evolution of the Star-Forming "Main Sequence" from z ˜ 0-6. *ApJS*, **214**, 15.

[118] Stil, J. M., M. Krause, R. Beck, and A. R. Taylor, 2009: The Integrated Polarization of Spiral Galaxy Disks. *ApJ*, **693**, 1392–1403.

[119] Sur, S., D. R. G. Schleicher, R. Banerjee, C. Federrath, and R. S. Klessen, 2010: The Generation of Strong Magnetic Fields During the Formation of the First Stars. *ApJL*, **721**, L134–L138.

[120] Tabatabaei, F. S., T. P. K. Martinsson, J. H. Knapen, J. E. Beckman, B. Koribalski, and B. G. Elmegreen, 2016: An Empirical Relation between the Large-scale Magnetic Field and the Dynamical Mass in Galaxies. *ApJL*, **818**, L10.

[121] Tasker, E. J., 2011: Star Formation in Disk Galaxies. II. The Effect Of Star Formation and Photoelectric Heating on the Formation and Evolution of Giant Molecular Clouds. *ApJ*, **730**, 11.

[122] Thomson, R. C. and A. H. Nelson, 1980: The interpretation of pulsar rotation measures and the magnetic field of the galaxy. *MNRAS*, **191**, 863–870.

[123] Turk, M. J., T. Abel, and B. O'Shea, 2009: The Formation of Population III Binaries from Cosmological Initial Conditions. *Science*, **325**, 601–.

[124] Turk, M. J., B. D. Smith, J. S. Oishi, S. Skory, S. W. Skillman, T. Abel, and M. L. Norman, 2011: yt: A Multi-code Analysis Toolkit for Astrophysical Simulation Data. *ApJS*, **192**, 9.

[125] Van Eck, C., J.-A. Brown, A. Shukurov, and A. Fletcher, 2014: Magnetic Fields in a Sample of Nearby Spiral Galaxies. *ArXiv e-prints*.

[126] Vazza, F., M. Brüggen, C. Gheller, S. Hackstein, D. Wittor, and P. M. Hinz, 2017: Simulations of extragalactic magnetic fields and of their observables. *ArXiv e-prints*.

[127] Vogelsberger, M., S. Genel, V. Springel, P. Torrey, D. Sijacki, D. Xu, G. Snyder, D. Nelson, and L. Hernquist, 2014: Introducing the Illustris Project: simulating the coevolution of dark and visible matter in the Universe. *MNRAS*, **444**, 1518–1547.

[128] Voit, G. M., G. L. Bryan, B. W. O'Shea, and M. Donahue, 2015: Precipitation-regulated Star Formation in Galaxies. *ApJL*, **808**, L30.

[129] Voit, G. M., G. Meece, Y. Li, B. W. O'Shea, G. L. Bryan, and M. Donahue, 2017: A Global Model for Circumgalactic and Cluster-core Precipitation. *ApJ*, **845**, 80.

[130] Walch, S., P. Girichidis, T. Naab, A. Gatto, S. C. O. Glover, R. Wünsch, R. S. Klessen, P. C. Clark, T. Peters, D. Derigs, and C. Baczynski, 2015: The SILCC (SImulating the LifeCycle of molecular Clouds) project - I. Chemical evolution of the supernova-driven ISM. *MNRAS*, **454**, 238–268.

[131] Wang, P. and T. Abel, 2009: Magnetohydrodynamic Simulations of Disk Galaxy Formation: The Magnetization of the Cold and Warm Medium. *ApJ*, **696**, 96–109.

[132] Wang, P., T. Abel, and R. Kaehler, 2010: Adaptive mesh fluid simulations on GPU. *NewA*, **15**, 581–589.

[133] Widrow, L. M., 2002: Origin of galactic and extragalactic magnetic fields. *Reviews of Modern Physics*, **74**, 775–823.

[134] Widrow, L. M., D. Ryu, D. R. G. Schleicher, K. Subramanian, C. G. Tsagas, and R. A. Treumann, 2012: The First Magnetic Fields. *Space Science Reviews*, **166**, 37–70.

[135] Wielebinski, R. and F. Krause, 1993: Magnetic fields in galaxies. *Astronomy and Astrophysics Review*, **4**, 449–485.

[136] Wise, J. H. and T. Abel, 2011: ENZO+MORAY: radiation hydrodynamics adaptive mesh refinement simulations with adaptive ray tracing. *MNRAS*, **414**, 3458–3491.

[137] Wise, J. H., T. Abel, M. J. Turk, M. L. Norman, and B. D. Smith, 2012: The birth of a galaxy - II. The role of radiation pressure. *MNRAS*, **427**, 311–326.